Doping-independent 120° magnetism in the quadruple perovskite CaMn₃V₄O₁₂

Fabio Denis Romero [1,*] Kunlang Ji,[2] Claire V. Colin,[1] and J. Paul Attfield[2]

[1]*Université Grenoble Alpes, CNRS, Institut Néel, 38000 Grenoble, France*
[2]*Center for Science at Extreme Conditions, The University of Edinburgh, Edinburgh EH9 3FD, United Kingdom*

The magnetic structure of high-pressure quadruple perovskite $CaMn_3V_4O_{12}$ was investigated using neutron powder diffraction data. Below $T_N = 54$ K, the $S = \frac{5}{2}$ Mn^{2+} spins adopt a 120° arrangement in kagome layers formed of second nearest neighbor A' sites. The V^{4+} electrons are itinerant and do not mediate the magnetic interactions as evidenced by the insensitivity of the magnetic structure to the valence of the vanadium cations in $AMn_3V_4O_{12}$ ($A = La^{3+}, Ca^{2+}$).

I. INTRODUCTION

The quadruple perovskite structure with general formula $AA'_3B_4O_{12}$ is a particular variant of the cubic perovskite structure which is capable of accommodating magnetic transition metal cations in the square-planar A' sites and octahedral B sites. These materials can show a wide range of interesting properties such as intersite charge transfer, Kondo physics, or Fermi liquid behavior with only minor structural variations [1–3].

Of particular interest are quadruple perovskite materials without localized B-site cation spins (when B is nonmagnetic or with itinerant electrons). As a result of several competing (comparable) interactions between the square-planar A' sites, a wide variety of unusual magnetic structures can be stabilized, such as the collinear G-like antiferromagnetic structure of $CaCu_3Ti_4O_{12}$, the different orthogonal orderings of $CaM_3Ti_4O_{12}$ (M = Fe, Co), or the multi-k ordering of $CaCo_3V_4O_{12}$ [4–9]. The wide variety of magnetic structures can be rationalized as originating from the need to minimize the geometric frustration in the kagome lattices formed by the A' sites along the body diagonal directions of the cubic structure [7].

The quadruple perovskite $LaMn_3^{2+}V_4^{3.75+}O_{12}$ offers the clearest visualization of the influence of these layers on the magnetic properties. Below $T_N \sim 44$ K, the Mn^{2+} spins adopt a 120° order within planes perpendicular to the cubic $\langle 111 \rangle$ direction [5]. The isostructural A site substituted material $CaMn_3^{2+}V_4^{4+}O_{12}$ has a transition at $T_N = 54$ K to an "antiferromagnetic state," but the magnetic structure has never been investigated [10].

In these materials the substitution of Ca^{2+} for La^{2+} changes the valence state of the vanadium cations from $+3.75$ to $+4$ [10]. In both materials, the A' sites are exclusively occupied by $S = 5/2$ Mn^{2+} cations [10]. In this paper we report the magnetic properties and structure of $CaMn_3^{2+}V_4^{4+}O_{12}$ determined from neutron powder diffraction.

II. EXPERIMENT

Samples of $CaMn_3V_4O_{12}$ were prepared from a suitable stoichiometric mixture of CaO (99.99%), MnO (99.99%), V_2O_3(99.99%), and V_2O_5(99.95%). The precursor powders were ground together using an agate mortar and pestle in an argon-filled glove box and placed inside platinum capsules. These were treated at 900 °C for 30 min under 9 GPa using a Walker-type multianvil press. The pressure was released slowly after quenching to room temperature. Laboratory x-ray powder diffraction data were collected using a Bruker D8 diffractometer.

Magnetization measurements were performed using a Quantum Design MPMS-XL SQUID magnetometer. Neutron powder diffraction measurements were carried out using the D1b diffractometer at the ILL neutron source in Grenoble, France from a sample contained in a vanadium can. A monochromatic neutron beam with a wavelength of 2.52 Å was obtained with a HOPG monochromator. In order to have sufficient material for significant neutron scattering, the products of six different synthesis runs were combined to yield a total mass of approximately 180 mg. Rietveld refinements of the nuclear and magnetic structures were carried out using the GSAS-II program and magnetic structure determination was performed using k-SUBGROUPSMAG implemented therein [11,12].

III. RESULTS

Laboratory x-ray powder diffraction data confirmed the formation of cubic (space group $Im\bar{3}$) $CaMn_3V_4O_{12}$. Zero field cooled and field cooled magnetization measurements contained a local maximum at $T \sim 54$ K, consistent with previous reports [Fig. 1(a)] [10]. A fit of the zero field cooled data to the Curie-Weiss law in the range 100–300 K yielded values of $C = 11.73$ emuK/mol and $\theta = -101.64$ K, consistent with previous reports and spin-only $S = 5/2$ Mn^{2+} [10].

Neutron powder diffraction data collected from $CaMn_3V_4O_{12}$ at 100 K, significantly above the magnetic transition temperature, could be well accounted for using

*fabio.denis-romero@neel.cnrs.fr

(a)

(b)
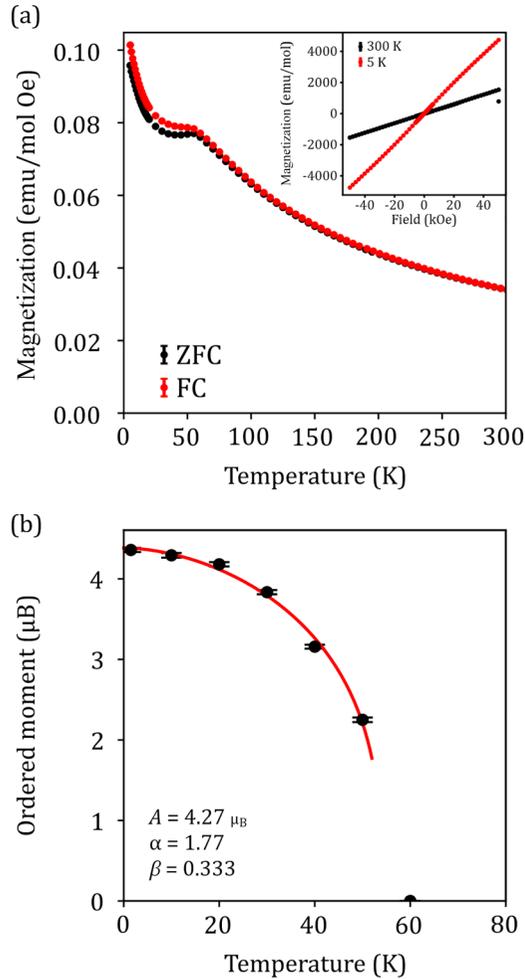
FIG. 1. (a) Zero field cooled (ZFC) and field cooled (FC) magnetization data collected as a function of temperature from $CaMn_3V_4O_{12}$. Inset: Magnetization as a function of field at 300 and 5 K. (b) Refined moment per Mn^{2+} cation as a function of temperature and the fit to a power law of the form $I = A[1 - (\frac{T}{T_N})^\alpha]^\beta$ with $T_N = 54$ K.

the cubic quadruple perovskite structure reported previously ($w_{Rp} = 2.69\%$) [10]. Observed, calculated, and difference plots are shown in Fig. 3(a) and the refined structural parameters are given in Table I. Attempts to vary the A' and B site occupancies did not result in any noticeable improvement

TABLE I. Parameters for the nuclear structure of $CaMn_3V_4O_{12}$ refined against neutron powder diffraction data collected at 100 K.

		$CaMn_3V_4O_{12}$ at 100 K			
Atom	x	y	z	Frac	U_{iso} (Å²)
Ca1	0	0	0	1	0.007
Mn1	0	1/2	1/2	1	0.007
V1	1/4	1/4	1/4	1	0.007
O1	0	0.197(1)	0.297(1)	1	0.007
		Space group: $Im\bar{3}$, $a = 7.404(1)$ Å			

to the fit, indicating the lack of any significant antisite disorder in this material.

Neutron powder diffraction data collected from $CaMn_3V_4O_{12}$ at 1.5 K contained additional reflections relative to the data collected at 100 K. These could be indexed on the basis of a magnetic propagation vector $k = [0, 0, 1]$. The data were well accounted for using the $R\bar{3}$ structure shown in Fig. 2(b). This magnetic cell is related to the nuclear cell by the transformation ($a_m = a_n - c_{n'} b_m = b_n + c_{n'} c_m = a_n - b_n + c_n$).

This magnetic structure is the same as that previously reported for $LaMn_3V_4O_{12}$ [5]. It consists of Mn spins arranged at $120°$ within the kagome planes formed by the A' sites along the $\langle 111 \rangle$ directions of the cubic nuclear cell (see Fig. 2). refinement of the magnetic structure was carried out using only a single parameter (M_X) and yielded a moment per Mn site of $4.42\mu_B$ [cf. 4.17(4) in $LaMn_3V_4O_{12}$], a good match for the $S = 5/2$ Mn^{2+} ($w_{Rp} = 3.34\%$) [5]. Observed, calculated, and difference plots are shown in Fig. 3(b) and the refined structural parameters are given in Table II. No evidence of peak splitting or broadening could be observed in the nuclear reflections, indicating that the cubic symmetry of the nuclear cell persists down to the lowest temperature measured.

Neutron powder diffraction data were collected at several other temperatures. A plot of the refined ordered moment as a function of temperature is shown in Fig. 1(b). A fit of these data to the phenomenological power law based on Landau theory of the form $I = A[1 - (\frac{T}{T_N})^\alpha]^\beta$ with $T_N = 54$ K yields values of $A = 4.27\mu_B$, $\alpha = 1.77$, and $\beta = 0.333$, in accordance with the value expected for a classical Heisenberg three-dimensional (3D) model ($\beta = 0.367$).

IV. DISCUSSION

At $T_N = 54$ K, $CaMn_3V_4O_{12}$ adopts a magnetic structure in space group $R\bar{3}$ with the Mn^{2+} spins lying in kagome planes parallel to the ab plane (perpendicular to the cubic $\langle 111 \rangle$ body diagonal of the nuclear cell). These are made up of networks of second nearest neighbor (2NN) A' cations. An equivalent 2NN exchange path exists between next nearest kagome layers, while adjacent kagome layers are instead linked by third nearest neighbor (3NN) interactions. In quadruple perovskite materials, first, second, third, and fourth nearest neighbor exchange interactions are typically comparable in energy, which contributes to the variety of nontrivial types of ordering seen in these phases. It has been noted previously that these structures are all different ways of relieving the inherent geometric frustration present in kagome layers with AFM interactions [7].

For the collinear G-like magnetic structures of $CaCu_3Ti_4O_{12}$ or $YMn_3Al_4O_{12}$, the spins within each layer are ferromagnetically aligned and adjacent layers couple antiferromagnetically [7,13,14]. This situation is realized when the interaction between 1NN spins is AFM and the interaction between 2NN is negligible ($J_1 < 0, J_2 \sim 0$). However, when the interaction between 2NN is AFM (i.e., $J_2 < 0$), we observe much more complex arrangements of spins. The $120°$ arrangement of spins within each layer observed in $AMn_3V_4O_{12}$ ($A =$ La, Ca) is a compromise solution.
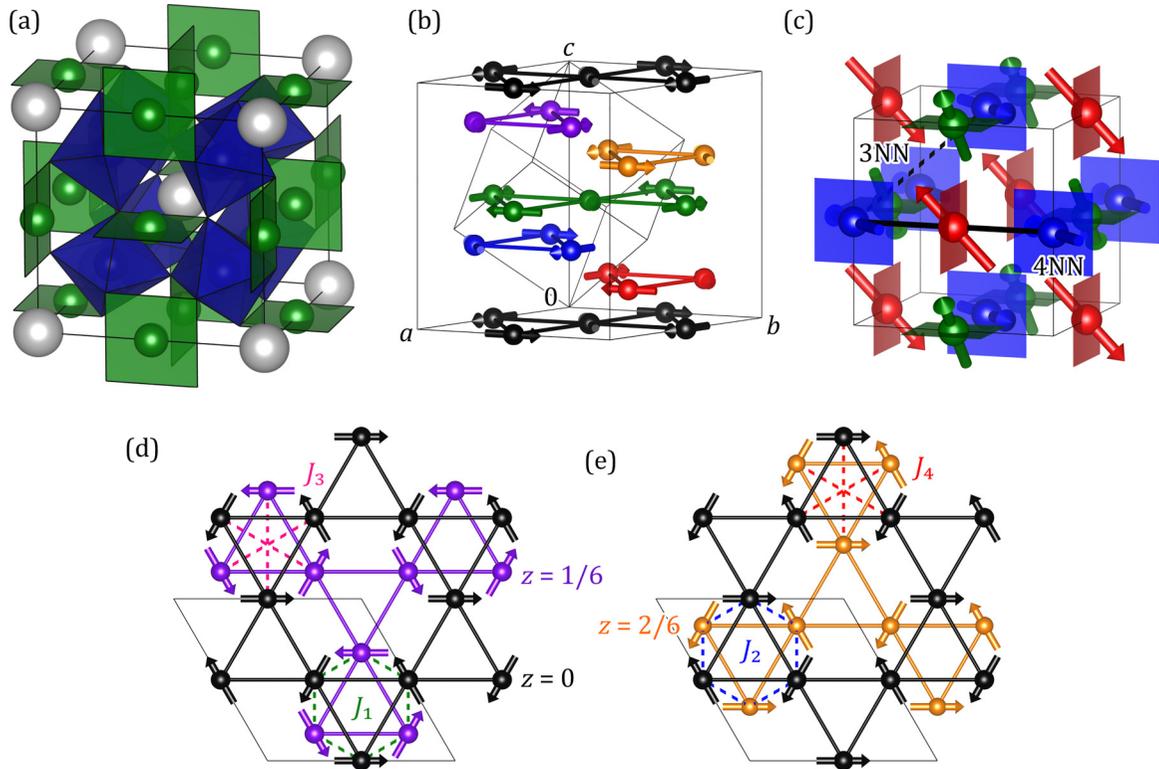
FIG. 2. (a) Nuclear structure of $CaMn_3V_4O_{12}$. (b) Rhombohedral magnetic structure of $CaMn_3V_4O_{12}$. The different colors correspond to the different kagome layers parallel to the rhombohedral ab plane. The cell edges of the original nuclear cubic cell are included. (c) Magnetic structure of $CaMn_3V_4O_{12}$ in the cubic setting highlighting the collinear ordering between spins which share a common orientation of the square-planar coordination environment. (d) Relation between two 1NN kagome planes along the ⟨111⟩ direction of the cubic nuclear cell. (e) Relation between two 2NN kagome planes along the ⟨111⟩ direction of the cubic nuclear cell.

One additional feature of quadruple perovskites worth considering is the orbital polarization of the A' sites. Interactions between sites with the same orbital polarization (orientation of the O_4 square-planar coordination environment) will be more significant than those between sites with orthogonal polarizations. In this structure type, 1NN and 2NN A' sites are orthogonally arranged, while 3NN and 4NN sites are parallel. This stabilizes, for example, the orthogonal order in $CaM_3Ti_4O_{12}$ which has long range structures consisting of three mutually orthogonal AFM sublattices each of which consists of the set of MO_4 square planes sharing a particular orientation [6,7]. In both cases, it is the long range 4NN interaction which is responsible for stabilizing the overall magnetic arrangement [6,7].

It should be noted that in this case, all Mn^{2+} sites which share a common orientation have collinear ordering [Fig. 2(c)]. The All 3NN interactions are AFM and all 4NN interactions are FM. In the resulting structure, thus, only the 2NN interaction is frustrated.

The magnetic structure reported herein is the same as that previously reported for the analogous material $LaMn_3V_4O_{12}$. The substitution of Ca for La results in a change in the average oxidation state of the V cations from +3.75 to +4 [10]. This change has minimal effect on the magnetic properties and both compounds have comparable T_N (44 and 54 K for La and Ca, respectively) and ordered moments (4.17 and $4.42\mu_B$) [10].

The T_N changes from 44 to 54 K, a change which is largely associated with a decrease in the unit cell volume on sub-

stitution $[a_{La} = 7.48485(4)$ Å, $a_{Ca} = 7.40704(3)$ Å at 300 K] [10]. In both compounds, the vanadium electrons are itinerant, giving rise to metallic conduction, and do not interact with the localized electrons at the Mn^{2+} sites. The lack of correlation between the magnetic and transport behavior in this family of materials opens up intriguing possibilities to tune different emergent properties independently.

The other reported members of the $CaM_3B_4O_{12}$ are summarized in Table III. While there are a number of oxides

TABLE II. Parameters for the nuclear and magnetic structures of $CaMn_3V_4O_{12}$ refined against neutron powder diffraction data collected at 1.5 K.

Atom	x/M_x	y/M_y	z/M_z	Frac	U_{iso} (Å²)
		$CaMn_3V_4O_{12}$ at 1.5 K			
Ca1	0	0	0	1	0.005
Mn1	1/2	0	0	1	0.005
	4.42(1)	0	0		
V1	1/2	0	1/4	1	0.005
V2	0	0	1/4	1	0.005
O1	0.966(1)	0.230(1)	0.034(1)	1	0.005
O2	0.835(1)	0.969(1)	0.164(1)	1	0.005

Space group: $R\bar{3}$
Space group: $R\bar{3}$, $a = 10.425(1)$ Å, $c = 12.864(1)$
[Pseudocubic $a = 7.402(1)$ Å]
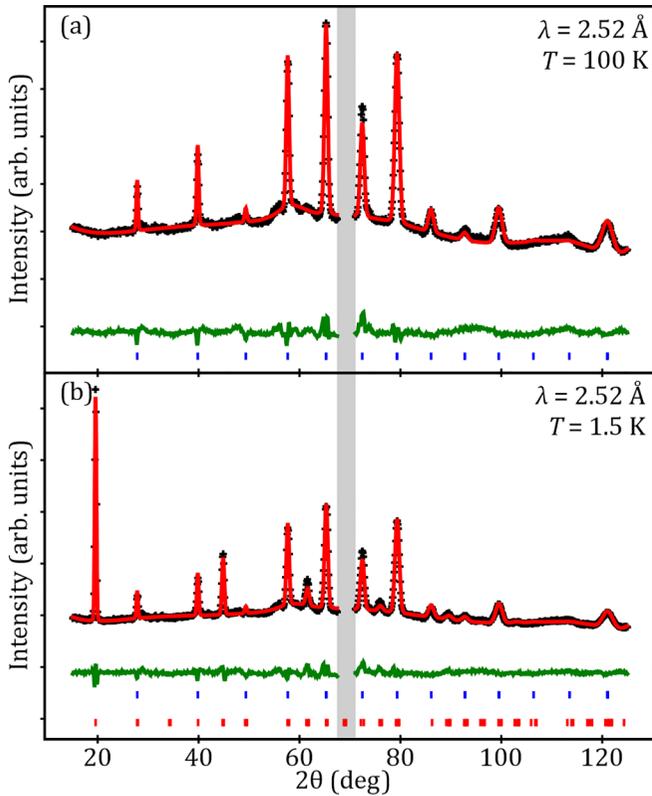
FIG. 3. Observed (black), calculated (red), and difference (green) plots for the refinements of $CaMn_3V_4O_{12}$ at (a) 100 K and (b) 1.5 K. The blue tick marks correspond to nuclear reflections and the red tick marks to magnetic reflections. The shaded region contains a contribution from the cryostat and the vanadium sample holder and was excluded during the refinement.

known with Ni^{2+} cations in square-planar environments, there are yet no examples of quadruple perovskite materials with Ni^{2+} at the A' sites. This is likely because of the high stability of NiO (and consequent unreactivity) at the high pressures typically required to stabilize these phases. Similarly, attempts to prepare $CaMn_3Ti_4O_{12}$ have so far resulted in the preferential formation of a mixture of $CaTiO_3$ and $MnTiO_3$ perovskites [15]. Attempts to prepare $CaFe_3V_4O_{12}$ at pressures $P \leqslant 8$ GPa produced a mixture of $(Fe/V)_2O_3$ and $CaVO_3$ while the solid solution limit for the system $CaCu_{3-x}Fe_xV_4O_{12}$ under these conditions is limited to $x \sim 1$ [16].

TABLE III. Selected magnetic and transport properties of the $CaM_3B_4O_{12}$ materials ($B = V^{4+}, Ti^{4+}$).

$CaM_3B_4O_{12}$ M =	$B = V^{4+}$	$B = Ti^{4+}$
Mn^{2+}	$T_N = 54$ K 120° order $k = (0, 0, 1)$ Metallic [10] (This work)	Not reported
Fe^{2+}	Not reported	$T_N = 2.8$ K Orthogonal AFM $[k = (\frac{1}{2}, \frac{1}{2}, 0)]$ [6] Insulator
Co^{2+}	$T_N = 100$ K Multi-k ordering [8,9] $k = (0, 0, 1)$ and $(0, 0, \frac{1}{2})$ Semimetal	$T_N = 9.3$ K Orthogonal AFM $[k = (\frac{1}{2}, \frac{1}{2}, \frac{2}{2})]$ [7] Insulator
Ni^{2+}	Not reported	Not reported
Cu^{2+}	Pauli paramagnet [17] Metallic	$T_N = 27$ K G-like AFM [4] $k = (0, 0, 0)$ Insulator

V. CONCLUSIONS

We carried out neutron powder diffraction measurements on $CaMn_3^{2+}V_4^{4+}O_{12}$ and determined its magnetic structure, finding a 120° arrangement as in $LaMn_3^{2+}V_4^{3.75+}O_{12}$ rather than the G-like arrangement found in $CaCu_3Ti_4O_{12}$ previously assumed [18,19]. The low-temperature magnetic behavior of these phases is independent of the average vanadium oxidation state, with only a change in T_N ascribable to chemical pressure exerted by a decrease in the lattice parameter. The lack of correlation between the magnetic and transport behavior in this family of materials opens up intriguing possibilities to tune different emergent properties independently via site-selective doping.

[1] I. Yamada, M. Murakami, N. Hayashi, and S. Mori, Inverse charge transfer in the quadruple perovskite $CaCu_3Fe_4O_{12}$, Inorg. Chem. **55**, 1715 (2016).

[2] D. Meyers *et al.*, Competition between heavy fermion and Kondo interaction in isoelectronic A-site-ordered perovskites, Nat. Commun. **5**, 5818 (2014).

[3] M.-R. Li *et al.*, Strong electron hybridization and Fermi-to-non-Fermi liquid transition in $LaCu_3Ir_4O_{12}$, Chem. Mater. **27**, 211 (2015).

[4] A. Collomb, D. Samaras, B. Bochu, and J. C. Joubert, Propriétés et structure magnétiques de $CaCu_3Ti_4O_{12}$ à structure pérovskite, Phys. Status Solidi **41**, 459 (1977).

[5] T. Saito, M. Toyoda, C. Ritter, S. Zhang, T. Oguchi, J. P. Attfield, and Y. Shimakawa, Symmetry-breaking 60°-spin order in the A-site-ordered perovskite $LaMn_3V_4O_{12}$, Phys. Rev. B **90**, 214405 (2014).

[6] M. A. Patino, F. D. Romero, M. Goto, T. Saito, F. Orlandi, P. Manuel, A. Szabó, P. Kayser, K. H. Hong, and K. N. Alharbi, Multi-k spin ordering in $CaFe_3Ti_4O_{12}$ stabilized by spin-orbit coupling and further-neighbor exchange, Phys. Rev. Res. **3**, 043208 (2021).

[7] M. A. Patino, F. D Romero, H.-J. Koo, M. Avdeev, S. D. A. Injac, M. Goto, M.-H. Whangbo, and Y. Shimakawa, Orthogonal antiferromagnetism to canted ferromagnetism in

CaCo$_3$Ti$_4$O$_{12}$ quadruple perovskite driven by underlying kagome lattices, Commun. Mater. **3**, 51 (2022).

[8] S. V. Ovsyannikov, Y. G. Zainulin, N. I. Kadyrova, A. P. Tyutyunnik, A. S. Semenova, D. Kasinathan, A. A. Tsirlin, N. Miyajima, and A. E. Karkin, New antiferromagnetic perovskite CaCo$_3$V$_4$O$_{12}$ prepared at high-pressure and high-temperature conditions, Inorg. Chem. **52**, 11703 (2013).

[9] S. V. Ovsyannikov *et al.*, Structural and magnetic transitions in CaCo$_3$V$_4$O$_{12}$, perovskite at extreme conditions, Inorg. Chem. **56**, 6251 (2017).

[10] S. Zhang, T. Saito, M. Mizumaki, W. Chen, T. Tohyama, and Y. Shimakawa, Site-selective doping effect in AMn$_3$V$_4$O$_{12}$ (A = Na$^+$, Ca^{2+}, and La^{3+}), J. Am. Chem. Soc. **135**, 6056 (2013).

[11] B. H. Toby and R. B. Von Dreele, GSAS-II: The genesis of a modern open-source all purpose crystallography software package, J. Appl. Crystallogr. **46**, 544 (2013).

[12] J. M. Perez-Mato, S. V. Gallego, E. S. Tasci, L. Elcoro, G. de la Flor, and M. I. Aroyo, Symmetry-based computational tools for magnetic crystallography, Annu. Rev. Mater. Res. **45**, 217 (2015).

[13] H. Li, X. Liu, C. Li, S. Lv, Y. Bai, Z. Wang, and J. Meng, Magnetic coupling mechanism in *A*-site ordered perovskite YMn$_3$Al$_4$O$_{12}$: Extended (Mn–O)–(O–Mn) superexchange, Solid State Sci. **17**, 63 (2013).

[14] Y. Shimakawa and T. Saito, *A*-site magnetism in *A*-site-ordered perovskite-structure oxides, Phys. Status Solidi B **249**, 423 (2012).

[15] N. L. Ross, J. Ko, and C. T. Prewitt, A new phase transition in MnTiO$_3$:LiNbO$_3$-perovskite structure, Phys. Chem. Miner. **16**, 621 (1989).

[16] N. I. Kadyrova, Yu. G. Zainulin, A. P. Tyutyunnik, N. V. Mel'nikova, and I. S. Ustinova, High-pressure/high-temperature synthesis, crystal structure, and electrical properties of CaCu$_{3-x}$Fe$_x$V$_4$O$_{12}$, Inorg. Mater. **47**, 1396 (2011).

[17] H. Shiraki, T. Saito, M. Azuma, and Y. Shimakawa, Metallic behavior in *A*-site-ordered perovskites AMn$_3$V$_4$O$_{12}$ with A = Na$^+$, Ca^{2+}, and Y^{3+}, J. Phys. Soc. Jpn. **77**, 064705 (2008).

[18] S. Zhang, T. Saito, W.-T. Chen, M. Mizumaki, and Y. Shimakawa, Solid solutions of Pauli-paramagnetic CaCu$_3$V$_4$O$_{12}$, and antiferromagnetic CaMn$_3$V$_4$O$_{12}$, Inorg. Chem. **52**, 10610 (2013).

[19] G. Zhang, Y. Wang, Z. Cheng, Y. Yan, C. Peng, C. Wang, and S. Dong, A class of rare antiferromagnetic metallic oxides: Double perovskite AMn$_3$V$_4$O$_{12}$ (A = Na$^+$, Ca^{2+}, and La^{3+}) and the site-selective doping effect, Phys. Chem. Chem. Phys. **17**, 12717 (2015).